Fluorescence polarization activity-based protein profiling on retaining glycosidases

Lahav, D.

5

Competitive Fluorescence Polarization Activity Based Protein Profiling allows the Discovery of New Golgi α-Mannosidase Inhibitors

5.1 Introduction

N-linked glycosylation is a complex and ubiquitous process in eukaryotic cells. The process commences in the endoplasmic reticulum (ER, Figure 1A). Here, *N*-glycans are added to secreted and membrane-bound glycoproteins at Asn-X-Ser/Thr sites, where X can be any canonical amino acid (except for proline), and in which the Asn residue gets glycosylated. The transfer of an *N*-glycan occurs at the luminal side of the ER during or after translocation of a nascent polypeptide. The *N*-glycans are further processed by glycosidases and glycosyltransferases both within the ER and the Golgi apparatus.[1] One of the key enzymes involved in *N*-glycoprotein processing is Golgi α-mannosidase 2 (GMII). GMII catalyzes the hydrolysis of two distinct mannosyl linkages within the $GlcNAcMan_5GlcNAc_2$ oligosaccharide fragment of a high-mannose type *N*-glycan, as depicted in Figure 1A.[1,2] Further maturation of the glycoproteins is realized by the addition of sugars to the *N*-glycan core, elongation of branched GlcNAc residues and addition of sulfates or phosphates to complex *N*-glycan branches, resulting in a myriad of complex *N*-glycans. Altered *N*-glycan branching has been directly linked to the facilitation of cancer progression, for instance, *N*-glycans have been observed to be more branched when the cells become more cancerous. Such altered *N*-glycosylation patterns were found in breast-, colon- and skin cancers.[3,4] Compounds able to interfere with *N*-glycan processing have for many years been considered for development as antitumor agents. The potent mannosidase inhibitor, swaisonine **1** (Figure 1B), a water-soluble indole alkaloid which was first isolated from locoweed[5], is able to stop tumor growth and metastasis in a number of cancer types.[6-10] However, swaisonine is not selective for GMII and also potently inhibits lysosomal α-mannosidase MAN2B1 (LAM). Inhibition of LAM results in symptoms that resemble the lysosomal storage disorder, α-mannosidosis.[11,12]

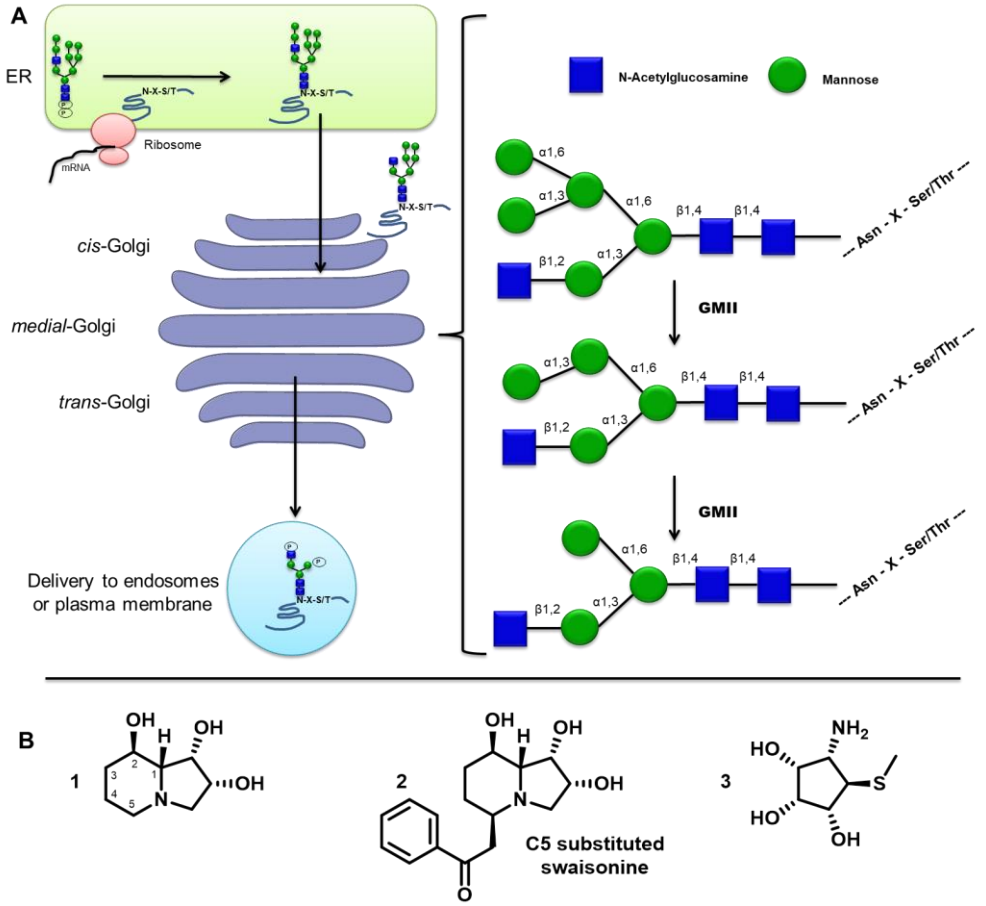

Figure 1. (A) Overview of processing and maturation of an N-glycan. GMII, present in the *medial* Golgi leaflet, catalyses the cleavage of two mannosyl linkages converting its substrate $GlcNAcMan_5GlcNAc_2$ into $GlcNAcMan_3GlcNAc_2$. (B) Chemical structures of swainsonine (**1**), C5 substituted swainsonine (**2**) and mannostatin A (**3**).

As GMII is a promising anti-cancer target, significant research has been devoted to identify or design new and selective GMII inhibitors. The modification of existing GMII inhibitors led to swainsonine derivatives containing C5-substituents (such as **2**), which show potent inhibitory potential for *Drosophila* GMII (dGMII; 40% identity to human GMII), but its selectivity over *Drosophila* lysosomal mannosidase (dLAM; 45% identity to human LAM) is modest.[1] The sequence similarity between human and drosophila α-mannosidases is high and the catalytic characteristics are found to be indistinguishable.[2] Another established α-mannosidase inhibitor, mannostatin A (**3**), was derivatized in a similar fashion. However these analogues had a reduced specificity for human GMII over human LAM.[13] Hydroxylated pyrrolidines were first identified by Popowycz *et al.*[14] and functionalized, hydroxylated pyrrolidines have

been shown to be more selective towards GMII. A different approach for the identification of inhibitors was performed by Kuntz *et al*.[15], who employed a fluorogenic substrate assay in screening a focused library containing potential glycosidase dGMII inhibitors. Despite these activities, no truly selective and potent GMII inhibitors have seen the light yet, hampering exploitation of this promising target towards the development of new anticancer agents. With the aim to identify new leads and following strategies outlined in the previous chapters, a fluorescence polarization activity-based protein profiling (FluoPol-ABPP) assay using a retaining α-mannosidase-selective activity-based probe (ABP) was developed. The results of this assay development, as well as screening of the in-house (Leiden University) focused library of glycomimetics are presented in this chapter.

5.2 Results and Discussion

The enzyme, GMII, a glycoside hydrolase family GH38 retaining α-mannosidase, processes its substrate employing a Koshland two-step, double displacement mechanism, as shown in Figure 2.

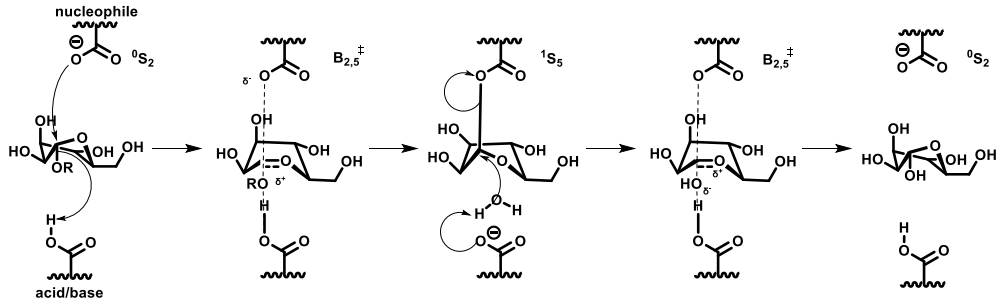

Figure 2. Proposed mechanism of substrate degradation by retaining α-mannosidase

Protonation and expulsion of the aglycon likely proceeds through a (near) boat conformation ($B_{2,5}$) in the transition state.[2] The probes described in the previous chapters are targeting the protein of interest based on their structural and conformational resemblance of the transition state. However, there are exceptions to these transition state mimetics. The α-mannopyranose-configured cyclophellitol preferably adopts a $^4H_3$ conformation, but is an effective inhibitor of jack bean α-mannosidase.[16] As has been discussed in the previous chapters, FluoPol-ABPP works best when red fluorescent dyes, such as tetra-aminomethylrhodamine (TAMRA) are used. With this reasoning in mind, the studies described in this

chapter commenced with the synthesis of TAMRA-modified α-mannopyranose-configured cyclophellitol aziridine **16** (Scheme 1).

5.2.1 Synthesis of α-mannosidase ABP 16

The synthesis of α-mannopyranose-configured cyclophellitol aziridine was accomplished following experimental procedures described by Madsen *et al.*[17], but using D-ribose instead of D-xylose (scheme 1) as the starting material. D-ribose was converted into benzyl protected furanoside (**4**) via Fisher glycosylation, tritylation of the primary alcohol, benzylation of the secondary alcohols and detritylation. The primary alcohol in the resulting **4** was converted to the iodide via an Appel reaction to give compound **5**. Zinc-mediated reductive fragmentation of **5** afforded **6**. Indium-mediated allyl addition using bromo-crotonate in the presence of lanthanide triflate yielded diastereomerically pure **7**. Diene **8** was obtained via ring-closing metathesis using Grubbs 2nd generation catalyst. The ester functionality in **8** was then reduced using DIBAL-H, affording diol **9**. In this step the addition of sodium borohydride and water was implemented in the workup, in order to avoid aldehyde contamination. Epoxidation of the diene moiety was realized using mCPBA, resulting in a mixture of α- and β-configured epoxides **10** and **11**. The free secondary alcohols in **10** were benzylated (NaH, BnBr), yielding fully protected epoxide **12**. The epoxide in **12** was transformed into α-configured aziridine **13** by treatment with sodium azide followed by treatment of the resulting mixture of 2-azido-alcohols with triphenylphosphine. Aziridine **13** was debenzylated via a Birch reaction, giving deprotected aziridine **14**. The aziridine moiety in **14** was alkylated with 1-iodo-8-azido-alkane under alkaline conditions to yield **15**. Copper(I) catalyzed azide-alkyne [2+3] cycloaddition of the azide in **15** with TAMRA-PEG$_4$-alkyne gave **16**, which was purified to homogeneity by HPLC.

Scheme 4: Synthetic route towards α-mannosidase ABP (**16**)

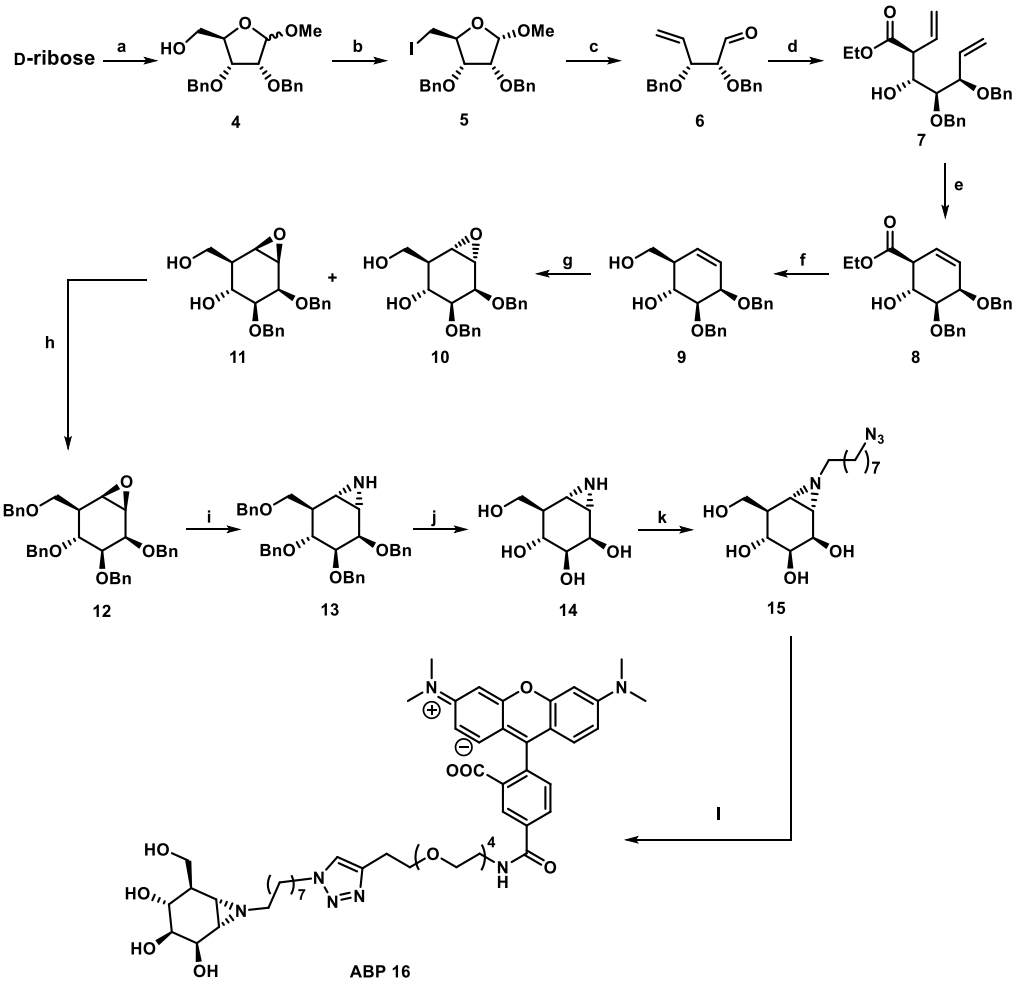

Reagents and conditions (a) i) AcCl, MeOH; ii) TrtCl, pyr, iii) BnBr, NaH, DMF; iv) pTsOH, MeOH, DCM, 72% (b) PPh_3, I_2, imidazole, THF, reflux, 93% (c) Zn, THF, H_2O, 40% (d) ethyl 4-bromocrotonate, $La(OTf)_3$, In, H_2O, 61% (e) Grubbs 2nd generation, DCM, reflux, 93% (f) i) DIBAL-H, THF, ii) EtOAc, H_2O, $NaBH_4$, 95% (g) mCPBA, DCE, reflux, 18% for **10**; 29% for **11** (h) **11**, BnBr, NaH, DMF, 52% (i) i) NaN_3, $LiClO_4$, MeCN, reflux, ii) PPh_3 polymer bound, MeCN, reflux, 54%; (j) Li, NH_3; (k) 1-azido-8-iodooctane, K_2CO_3, DMF, 80°C, 38% (l) 5'/6'-TAMRA-alkyne, CuI and THPTA in DMF, 48h, ambient temperature, 44%.

5.2.2 Compound 16 is an α-mannosidase probe

The initial *in vitro* experiments that were performed with probe **16** served to establish its ability to identify retaining α-mannosidases from complex biological samples. Recombinant α-mannosidase from jack bean (1 µg) was treated with 5 µM probe and this mixture was incubated for 30 minutes at 37°C. The pH of the McIlvaine buffer was varied from 3.0 to 7.0 within this experiment in order to

evaluate the degree of labelling at different pH-values. A similar experiment was conducted on extracts of mouse testis (5 µg protein content), containing potentially all five retaining α-mannosidases expressed in this tissue (enzymes homologous to the five known human retaining α-mannosidases). The five known human α-mannosidases from the Glycoside Hydrolase Family 38 (GH38) as listed in the carbohydrate active enzymes (CAZY) database are: α-mannosidase II (Man2A1; mouse 132 kDa), α-mannosidase a (lysosomal Man2B1; mouse 115 kDa), α-mannosidase IIx (Man2A2; mouse 132 kDa), neutral α-mannosidase (Man2C1; mouse 116 kDa) and α-1,6-mannosidase (Man2B2; mouse 116 kDa). The degree of labelling on these mannosidases was also evaluated by varying the pH, and labeling could be blocked by treatment with excess (25 µM) of the non-tagged inhibitor **1** prior to adding ABP **16** (5 µM) (lanes 2, 4 6, 8, 10, 12 and 14). After probe treatment, all samples were denatured by adding sodium dodecylsulfate (SDS) and heating to 100°C. The samples containing the thus denatured proteins were separated by gel electrophoresis. The wet gel slabs were scanned for fluorescence and the resulting signals were recorded. As shown in Figure 3A the fluorescent signal corresponds to the two different monomers from jack bean α-mannosidase (about 44 and 66 kDa). From Figure 3B it appears that the probe is able to label different α-mannosidases by varying the pH and that the labelling is blocked when the samples were pre-incubated with an excessive amount of **1**. Based on these results in can be concluded that ABP **16** is a viable α-mannosidase activity-based probe.

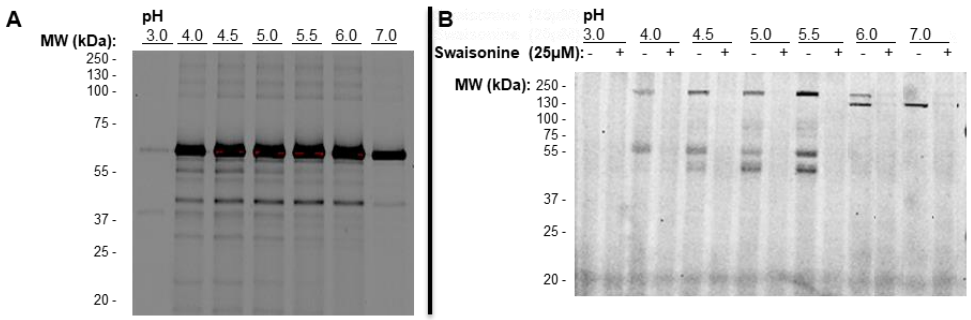

Figure 3. ABPP on (A) jack bean mannosidase and (B) mouse testis tissue using ABP **16** (5 µM).

5.2.3 ABP 16 is a viable FluoPol-ABPP probe

As depicted in Figure 4A, probe bound to the enzyme should give rise to a high FluoPol signal whereas unbound probe should return largely depolarized light upon

excitation. The FluoPol-ABPP experiments were conducted with 100 nM purified GMII from drosophila (dGMII) in a 384-well format (V_{final} = 25 µL). The wells were preloaded with (concentrated) dGMII and subsequently dissolved in a specific buffer containing 0.1% (w/v) bovine serum albumin (BSA), 0.5 mg/mL Chaps (detergent) and 1 mM $ZnSO_4$. The FluoPol signal was monitored over time after the addition of ABP **16**. The maximal polarization signal was obtained after 18h. Initially the probe concentration was optimized and it was found that the largest window, that is, difference in FluoPol-signal between bound and unbound probe, was realized when using 25 nM probe (Figure 4B). In addition, it was observed that the optimal window after 18h was obtained when performing the FluoPol assay with 100 mM MES buffer at pH 6.5 (Figure 4B). Positive controls contained an excessive amount of **1** and samples without inhibitors were considered as negative controls. Compounds **1** and **3** showed a dose-dependent inhibitory response in the FluoPol assay (Figure 4B). The IC_{50}-values of **1** and **3** were determined using the FluoPol-ABPP assay and found equal to respectively 30 nM and 96 µM. The observed potency of **1** (IC_{50} = 70 nM)[18] is in line with the literature, while **3** (IC_{50} = 70-160 nM)[18] is significantly higher.

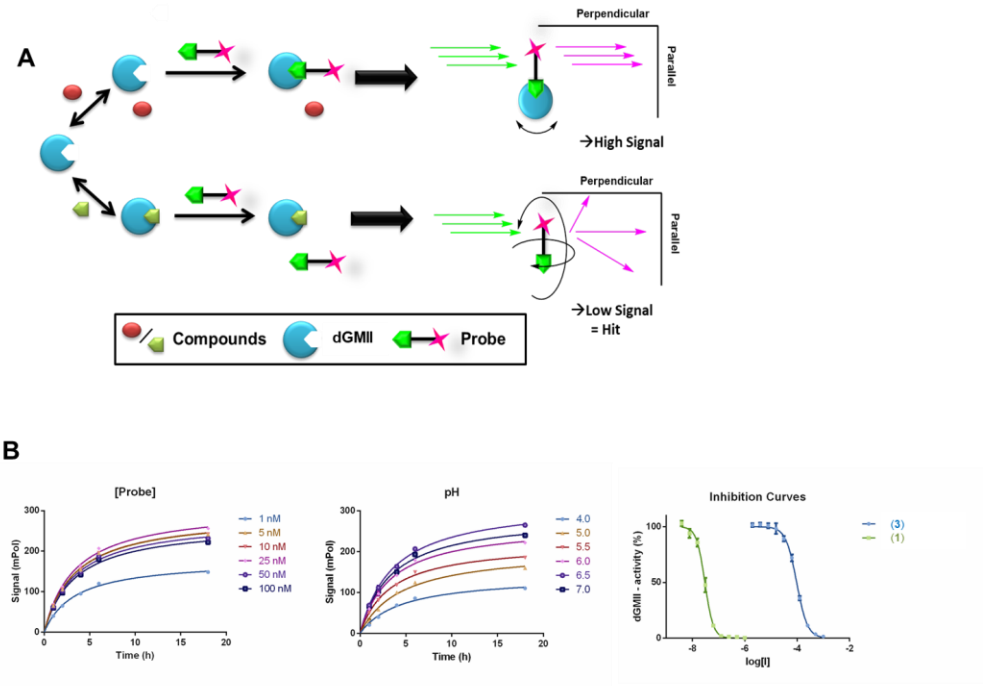

Figure 4. (A) Schematic representation of FluoPol-ABPP assay on dGMII. (B) From left to right; effect of probe concentration and pH on FluoPol-signal and in the final graph presenting a dose-dependent response of **1** and **3** on dGMII.

5.2.4 FluoPol-ABPP yields new GMII inhibitors

After optimization of the assay conditions, the iminosugar library also used in the previous chapters (see Appendix) was screened for its inhibitory potential on dGMII. The inhibitory potential of in total 358 compounds were assessed at a concentration of 5 µM, and compounds were pre-incubated with 100 nM dGMII for 30 minutes at 37°C. The final volume of the reactions in the screen was set at 15 µL per well and the polarization signal was measured 18h after treatment with ABP **16**. The residual dGMII-activities were calculated from the FluoPol-data and subsequently plotted against the compounds (Figure 5A). Seven compounds, depicted in Figure 5B, were able to reduce dGMII activity with more than 20% according to the FluoPol data.

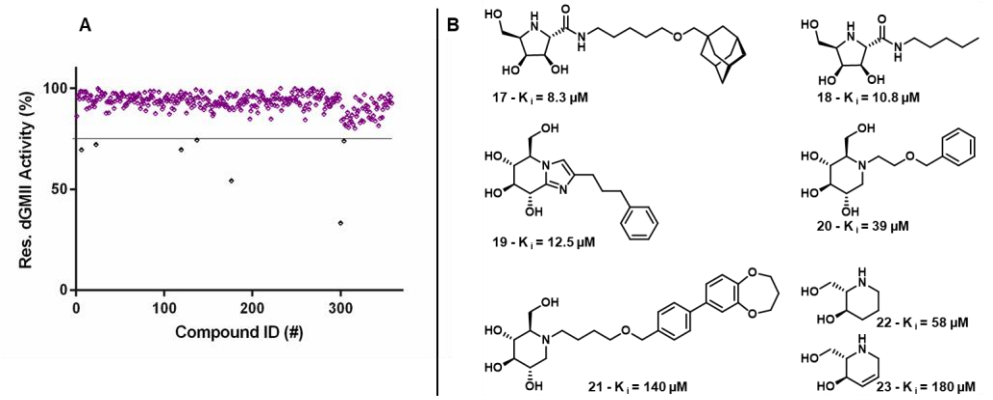

Figure 5. (A) Screening of an in-house library containing 350+ entries at a concentration of 5 µM on dGMII using FluoPol-ABPP. (B) Chemical structures of the seven hits including the K_i determined using the fluorogenic method described by Kuntz *et al.*[19]

The two lipophilic D-*lyxo*-pyrollidines (**17**) and (**18**) proved to be the most potent dGMII inhibitors of all compounds tested. The K_i-values were determined in a fluorogenic substrate assay using α-methylumbelliferylmannopyranoside as the fluorogenic substrate (see for the results from this assay, Table 1). The potency of the two *lyxo*-configures pyrrolizidines on dGMII are approximately 10 µM according to this orthogonal assay.

Table 1. K_i and IC_{50} values for the identified mannosidase inhibitors.

Inhibitor	*dGMII IC_{50} (μM)*[a]	*dGMII K_i (μM)*[b]
17	6.1	8
18	8.7	10.8
19	49.7	140
20	18.0	12.5
21	17.7	58
22	55.6	180
23	21.8	39

[a] Determined via FluoPol-ABPP assay

[b] Determined by initial rates of hydrolysis 4MU-alfa-Man in the presence of inhibitor

To understand the mode of action of the seven new (modest to rather potent) GMII inhibitors, the structure of their complex with dGMII were solved by crystallography, Figure 6 data obtained by collaborating with Zachary Armstrong and Gideon Davies, University of York, UK. All seven inhibitors were found to interact with the active site of dGMII and coordinate with the zinc ion present in the enzyme active site. Both 2- and 3-hydroxyls of **17** and **18** coordinate with the active site zinc, whereas hydroxylated piperidines **22** and **23** have only one hydroxyl coordinating to the active site zinc.

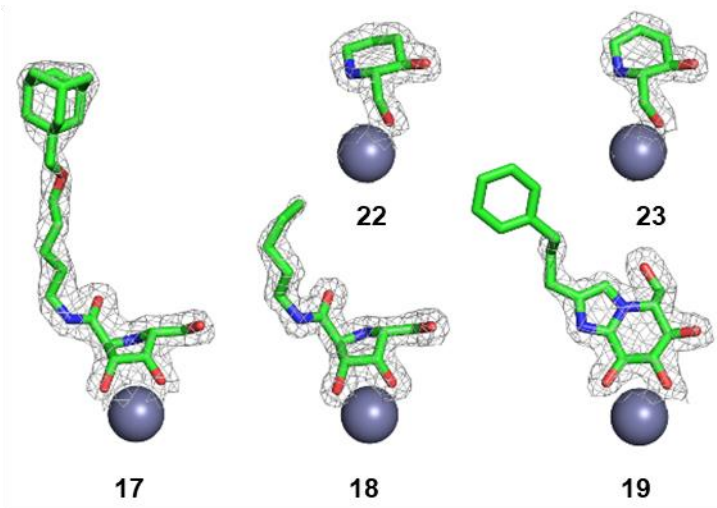

Figure 6. Crystal structures of **17**, **18**, **19**, **22** and **23** bound to dGMII. The zinc ion is depicted as a silver dot. For clarity only the compounds with zinc ion are depicted without the enzyme complex around it.

5.3 Conclusion

This chapter describes the synthesis of an α-mannopyranose-configured FluoPol compatible probe, ABP **16**, which was used for the development of an FluoPol based ABPP-assay for the identification of new GMII inhibitors. The FluoPol-ABPP assay has the required characteristics; low enzyme and probe requirements, and allows to easily discriminate between positive and negative controls. From the screen of the iminosugar based compound library, only seven compounds were identified to (weakly to rather potently) inhibit GAA and studied further. Two lipophilic D-*lyxo*-pyrollidines, two dihydroxylated piperidines, two deoxynojirimycins and one alkylated glycoimidazole were validated as GMII inhibitors in an orthogonal assay (for which a fluorogenic substrate assay was employed) and subsequent X-ray crystallography of these compounds bound to dGMII revealed new binding modes and potential sites for inhibitor diversification. This work could lead to the future development of selective GMII inhibitors, forming the basis of a new generation of chemotherapeutic agents. In addition, it is conceivable that due to the low expenses in terms of both enzyme and substrate usage during the developed FluoPol-ABPP assay, also other α-mannosidases, which may only be expressed in small quantities, could be screened. The latter should enable the screening for inhibitors of all human retaining α-mannosidases.

5.4 Experimental section

Chemicals, materials and methods

All solvents and reagents were obtained commercially and used as received unless stated otherwise. In contrast to previous chapters, the fluorophore, i.e. TAMRA, was purchased from Bio-Connect. Dichloromethane (DCM), dimethylformamide (DMF), tetrahydrofuran (THF) and methanol (MeOH) were dried over molecular sieves (4Å/3Å) for at least 12 hours before use. Reactions were monitored by TLC analysis using sheets with pre-coated silica with detection by UV-absorption (254 nm) wherever applicable and by spraying with 20% H_2SO_4 in MeOH, an aqueous solution containing $KMnO_4$ (5 g/L) and K_2CO_3 (95 g/L) or a solution of ninhydrin (6 g/L) in AcOH:MeOH (1:9, v/v) followed by charring at ≈ 200°C. Flash column chromatography was performed on silica gel (40-63 µm). For LC/MS analysis a HPLC-system (detection simultaneously at 213 nm, 254 nm and evaporative light detection) equipped with an analytical C-18 column (4.6 mmD × 250 mmL, 5 µ particle size) in combination with buffers A: H_2O, B: acetonitrile, C: 1.0% aqueous trifluoroacetic acid and coupled with an electrospray interface (ESI) was used. For

RP-HPLC purifications, an automated HPLC system equipped with a semi-preparative S2 C18 column (5 µm C18, 10Å, 150 × 21.2 mm) was used. The applied buffers were A: H2O + trifluoroacetic acid (1%) and B: MeCN. HPLC-MS purification was performed on an Agilent Technologies 1200 series automated HPLC system with a Quadropole MS 6130, equipped with a semi-preparative Gemini C18 column (Phenomex, 250 × 10, 5 µm) using buffers A: H_2O + K_2CO_3 (1%) and B: MeCN. Compounds were characterized by ^{1}H NMR-, ^{13}C NMR-, COSY- and HSQC NMR experiments. NMR spectra were recorded on a Bruker DPX-300, AV-400, AV-500 and AV-600 spectrometer in mentioned solvent. Chemical shifts are given in ppm (δ) relative to tetramethylsilane or the deuterated solvent as the internal standard. High-resolution mass spectra were recorded by direct injection (2 µL of a 2 µM solution in water/acetonitrile/tert-butanol, 1:1:1, v/v) on a mass spectrometer (Thermo Finnigan LTQ Orbitrap) equipped with an electrospray ion source with resolution R = 60000 at m/z 400 (mass range m/z = 150-2000).

((2R,3R,4R,5S)-3,4-bis(benzyloxy)-5-methoxytetrahydrofuran-2-yl)methanol (4)

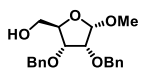

To a 0°C cooled solution of d-ribose (37.5 g, 250 mmol) in MeOH (500 mL) was added dropwise AcCl (3.5 mL, 50 mmol) and the reaction mixture was allowed to warm to room temperature. After complete conversion of the starting material the reaction was quenched with Et_3N till pH ≥7 and the mixture was concentrated *in vacuo* giving OMe-ribose as an α/β mixture (1:0.3). The crude OMe-ribose was co-evaporated with toluene and dissolved in pyridine (500 mL). To the solution was added trityl chloride (76.7 g, 275 mmol) and the mixture was stirred overnight at room temperature. The reaction was quenched with MeOH and the mixture was concentrated *in vacuo*. The product was dissolved in EtOAc and the organic phase was washed with H_2O (3x), brine (2x), dried over $MgSO_4$, filtered and concentrated *in vacuo*. The crude tritylated OMe-ribose was taken up in DMF (1 L) and to the solution was added BnBr (90 mL, 750 mmol) and the mixture was cooled to 0°C. To the cooled mixture was added (60%) NaH (25 g, 625 mmol) in small portions over a period of 6h. The reaction was gradually allowed to warm to room temperature and stirred overnight. The reaction mixture was cooled to 0°C and quenched with MeOH after which the solvents were removed *in vacuo.* The product was dissolved in Et_2O and the organic phase was washed with H_2O (3x), brine (2x), and dried over $MgSO_4$. The crude was filtered over silica, concentrated and dissolved in DCM/MeOH (1:1) (1 L). To the solution was added *p*TsOH (4.8 g, 25 mmol) and the reaction mixture was stirred overnight at room temperature. The mixture was neutralized with Et_3N and concentrated *in vacuo*. Purification by column chromatography (4/1 → 1/1,

pentane/EtOAc, v/v) yielded benzylated OMe-ribose as colorless oil (57.4 g, 179 mmol, 72%). Spectroscopic data were in accordance with literature.[22] (α-product) ^{1}H NMR (400 MHz, $CDCl_3$) δ 7.40 – 7.23 (m, 10H), 4.88 (s, 1H), 4.65 (d, *J* = 12.0 Hz, 1H), 4.60 (d, *J* = 12.0 Hz, 1H), 4.56 (d, *J* = 11.7 Hz, 1H), 4.47 (d, *J* = 11.7 Hz, 1H), 4.27 (dt, *J* = 6.9, 3.4 Hz, 1H), 4.11 (dd, *J* = 7.0, 4.7 Hz, 1H), 3.85 (d, *J* = 4.7 Hz, 1H), 3.78 (d, *J* = 12.2 Hz, 1H), 3.55 (ddd, *J* = 10.9, 7.3, 3.5 Hz, 1H), 3.34 (s, 3H), 2.15 (s, 1H). ^{13}C NMR (100 MHz, $CDCl_3$) δ 137.7, 137.7, 128.5, 128.0, 127.9, 127.9, 106.8, 82.3, 80.1, 77.3, 72.7, 72.5, 62.8, 55.6. (β-product) ^{1}H NMR (400 MHz, $CDCl_3$) δ 7.41 – 7.27 (m, 10H), 4.85 (d, *J* = 4.1 Hz, 1H), 4.74 (d, *J* = 12.7 Hz, 1H), 4.66 (d, *J* = 12.3 Hz, 1H), 4.65 – 4.54 (m, 2H), 4.17 (q, *J* = 3.5 Hz, 1H), 3.84 (dd, *J* = 6.9, 3.5 Hz, 1H), 3.73 (dd, *J* = 6.9, 4.2 Hz, 1H), 3.63 (dd, *J* = 12.0, 3.3 Hz, 1H), 3.45 (s, 3H), 3.39 (dd, *J* = 12.7, 3.5 Hz, 1H), 1.97 (s, 1H). ^{13}C NMR (100 MHz, $CDCl_3$) δ 138.2, 137.8, 128.4, 128.4, 128.2, 128.0, 127.9, 127.8, 102.7, 83.2, 78.1, 74.7, 72.7, 72.6, 62.7, 55.6.

(2S,3S,4R,5S)-3,4-bis(benzyloxy)-2-(iodomethyl)-5-methoxytetrahydrofuran (5)

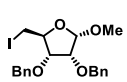

To a solution of benzylated α-OMe-ribose **4** (51.7 g, 113.8 mmol) in THF (455 mL) was added imidazole (15.5 g, 227.6 mmol), Ph_3P (44.8 g, 170.7 mmol) and the mixture was heated till reflux. A 1M I_2 solution (170.7 mL, 170 mmol) in THF was added dropwise to the boiling reaction mixture and refluxed overnight. The mixture was cooled to room temperature and Et_2O was added, upon addition of Et_2O crystalline precipitate was formed. The mixture was cooled to -20°C and the solids were filtered. The filtrate was washed with 10% $Na_2S_2O_3$ (aq.) (2x), H_2O (3x), brine (2x) dried over $MgSO_4$, filtered and concentrated *in vacuo*. The crude was immobilized on silica and purification by column chromatography (4/1, pentane/EtOAc, v/v) yielded iodo ribose as colorless oil (47.8 g, 105.4 mmol, 93%). Spectroscopic data were in accordance with literature.[23] ^{1}H NMR (300 MHz, $CDCl_3$) δ 7.34 – 7.28 (m, 10H), 4.92 (s, 1H), 4.65 (d, *J* = 11.7 Hz, 1H), 4.57 (d, *J* = 12.0 Hz, 1H), 4.57 (d, *J* = 12.0 Hz, 1H), 4.48 (d, *J* = 12.0 Hz, 1H), 4.14 (t, *J* = 6.6 Hz, 1H), 3.94 (dd, *J* = 6.6, 4.5 Hz, 1H), 3.88 (d, *J* = 4.5 Hz, 1H), 3.38 – 3.33 (m, 4H), 3.26 (dd, *J* = 10.5, 6.0 Hz, 1H). ^{13}C NMR (75 MHz, $CDCl_3$) δ 137.7, 128.6, 128.1, 128.0, 106.3, 81.8, 20.4, 80.2, 72.7, 72.5, 55.4, 8.8.

(2R,3R)-2,3-bis(benzyloxy)pent-4-enal (6)

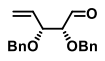

Iodo ribose **5** (47.8 g, 105.4 mmol) was dissolved in THF/H_2O (9:1) (1 L) and the solution was purged with argon under sonication. To the solution was added activated zinc (65.4 g, 1.0 mol) and the mixture was further sonicated at 60°C under argon atmosphere. After complete conversion of the starting material the excess of zinc was filtered and rinsed with DCM. The crude mixture was diluted

with brine and the product was extracted with DCM (5x). The combined organic phase was dried over $MgSO_4$, filtered and concentrated *in vacuo*. Purification by column chromatography (10/1, pentane/EtOAc, v/v) yielded the aldehyde as colorless oil (12.47 g, 42 mmol, 40%). Spectroscopic data were in accordance with literature.[24] ^{1}H NMR (400 MHz, $CDCl_3$) δ 9.63 (d, *J* = 2.1 Hz, 1H), 7.39 – 7.24 (m, 10H), 5.87 (dt, *J* = 17.6, 10.5, 7.6 Hz, 1H), 5.38 (d, *J* = 9.1 Hz, 1H), 5.34 (d, *J* = 16.9 Hz, 1H), 4.69 (d, *J* = 12.0 Hz, 1H), 4.64 (d, *J* = 12.2 Hz, 2H), 4.40 (d, *J* = 12.0 Hz, 1H), 4.16 (dd, *J* = 7.6, 4.6 Hz, 1H), 3.89 (dd, *J* = 4.6, 2.2 Hz, 1H). ^{13}C NMR (100 MHz, $CDCl_3$) δ 201.7, 137.8, 137.3, 134.1, 128.6, 128.5, 128.1, 127.8, 120.2, 85.0, 80.3, 73.1, 70.6.

Ethyl (2S,3R,4S,5R)-4,5-bis(benzyloxy)-3-hydroxy-2-vinylhept-6-enoate (7)

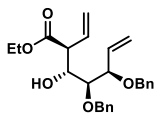

To a solution of aldehyde **6** (1.01 g, 3.41 mmol) in H_2O (15.4 mL) was added 75% ethyl 4-bromocrotonate (2.04 mL, 11.1 mmol), $La(OTf)_3$ (4.00 g, 6.83 mmol), indium powder (0.90 g, 7.85 mmol) and the mixture was vigorously stirred overnight at room temperature. The reaction mixture turned into a white slurry. The mixture was filtered over a pad of celite and rinsed with Et_2O. The layers were separated and the aqueous layer was extracted with Et_2O (3x). The combined organic phase was washed with H_2O (3x), brine (3x), dried over $MgSO_3$, filtered and concentrated *in vacuo*. Purification by column chromatography (9/1, pentane/EtOAc, v/v) yielded the diene as colorless oil (0.853 g, 2.078 mmol, 61%). ^{1}H NMR (400 MHz, $CDCl_3$) δ 7.37 – 7.26 (m, 10H), 5.89 (ddd, *J* = 17.5, 10.4, 7.2 Hz, 1H), 5.72 (ddd, *J* = 17.1, 10.3, 9.4 Hz, 1H), 5.41 (dt, *J* = 9.2, 1.3 Hz, 1H), 5.37 (t, *J* = 1.2 Hz, 1H), 5.14 (dd, *J* = 10.3, 1.4 Hz, 1H), 5.08 (d, *J* = 17.1 Hz, 1H), 4.68 (d, *J* = 11.2 Hz, 1H), 4.64 (d, *J* = 11.7 Hz, 1H), 4.44 (d, *J* = 11.3 Hz, 1H), 4.40 (d, *J* = 11.7 Hz, 1H), 4.24 (ddd, *J* = 9.5, 6.8, 1.3 Hz, 1H), 4.17 (t, *J* = 6.6 Hz, 1H), 4.13 (q, *J* = 7.3 Hz, 2H), 3.44 (dd, *J* = 5.8, 1.3 Hz, 1H), 3.34 (t, *J* = 9.5 Hz, 1H), 3.14 (d, *J* = 6.9 Hz, 1H), 1.24 (t, *J* = 7.1 Hz, 3H). ^{13}C NMR (100 MHz, $CDCl_3$) δ 172.6, 137.9, 137.9, 135.5, 133.1, 128.5, 128.5, 128.1, 128.0, 128.0, 127.8, 120.0, 119.6, 80.2, 79.0, 73.2, 72.0, 71.0, 60.9, 55.0, 14.2. HRMS: found 411.2165 $[M+H]^+$, calculated for $[C_{25}H_{30}O_5+H]^+$ 411.2166.

Ethyl(1S,4R,5S,6R)-4,5-bis(benzyloxy)-6-hydroxycyclohex-2-ene-1-carboxylate(8)

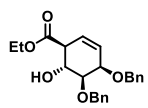

To a solution of diene **7** (0.575 g, 1.4 mmol) in DCM (56 mL) was added Grubbs 2nd generation catalyst (95 mg, 0.11 mmol, 8 mol%) and the reaction mixture was refluxed in the dark for 2 h. The mixture was concentrated *in vacuo* and purified by column chromatography (3/1, pentane/EtOAc, v/v) yielding the cyclohexene ethyl ester as

brown oil (0.498 g, 1.302 mmol, 93%). ^{1}H NMR (400 MHz, $CDCl_3$) δ 7.40 – 7.27 (m, 10H), 5.89 (ddd, *J* = 9.9, 5.2, 2.8 Hz, 1H), 5.82 (dd, *J* = 9.9, 2.4 Hz, 1H), 4.74 (d, *J* = 11.9 Hz, 1H), 4.69 (s, 2H), 4.62 (d, *J* = 11.8 Hz, 1H), 4.55 (ddd, *J* = 10.4, 8.8, 1.8 Hz, 1H), 4.21 (qd, *J* = 7.1, 0.8 Hz, 2H), 4.09 (t, *J* = 4.4 Hz, 1H), 3.46 (dd, *J* = 10.2, 4.0 Hz, 1H), 3.13 (ddt, *J* = 8.9, 2.5, 0.9 Hz, 1H), 2.91 (d, *J* = 1.9 Hz, 1H), 1.28 (t, *J* = 7.1 Hz, 3H). ^{13}C NMR (100 MHz, $CDCl_3$) δ 171.6, 138.6, 138.1, 128.6, 128.5, 128.1, 128.0, 128.0, 127.8, 127.5, 126.7, 80.3, 72.2, 71.9, 69.6, 67.3, 61.4, 51.2, 14.3. HRMS: found 383.1854 $[M+H]^+$, calculated for $[C_{23}H_{26}O_5+H]^+$ 383.1853.

(1R,2R,5R,6S)-5,6-bis(benzyloxy)-2-(hydroxymethyl)cyclohex-3-en-1-ol (9)

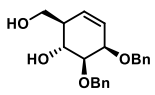

To a 0°C cooled solution of cyclohexene ethyl ester **8** (0.463 g, 1.2 mmol) in THF (40 mL) was added a 1M DIBAL-H sol. (6 mL, 6 mmol) in THF dropwise and the mixture was warmed to room temperature. After 30 min the mixture was cooled to 0°C and to the mixture was added EtOAc (2.4 mL, 24.4 mmol), H_2O (1.2 mL) and $NaBH_4$ (0.295 g, 7.8 mmol) in small portions. After stirring for 20 min at 0°C TLC showed full conversion of the starting material and the mixture was diluted with EtOAc. The mixture was transferred to a separation funnel and H_2O was added giving a white slurry. 1M HCl (aq.) was added till a clear two phase system was formed. The layers were separated and the aqueous layer was extracted with EtOAc (3x). The combined organic phase was washed with sat. $NaHCO_3$ (aq.), H_2O (3x), brine (3x), dried over $MgSO_4$, filtered and concentrated *in vacuo*. Purification by column chromatography (3/2 → 1/1, pentane/EtOAc, v/v) yielded the product as a white amorphous solid. (0.387 g, 1.137 mmol, 95%). ^{1}H NMR (600 MHz, $CDCl_3$) δ 7.39 – 7.27 (m, 10H), 5.88 (ddd, *J* = 9.9, 5.3, 2.8 Hz, 1H), 5.64 (dd, *J* = 9.9, 2.3 Hz, 1H), 4.72 (d, *J* = 11.6 Hz, 1H), 4.68 (d, *J* = 12.3 Hz, 1H), 4.67 (d, *J* = 12.1 Hz, 1H), 4.52 (d, *J* = 11.7 Hz, 1H), 4.13 – 4.08 (m, 2H), 3.81 – 3.73 (m, 2H), 3.46 (dd, *J* = 10.2, 3.9 Hz, 1H), 2.97 (s, 1H), 2.64 (s, 1H), 2.44 – 2.37 (m, 1H). ^{13}C NMR (150 MHz, $CDCl_3$) δ 138.6, 137.9, 130.7, 128.7, 128.5, 128.1, 128.1, 128.1, 127.9, 81.1, 71.8, 71.7, 70.1, 69.4, 65.9, 46.6. HRMS: found 341.1750 $[M+H]^+$, calculated for $[C_{21}H_{24}O_4+H]^+$ 341.1747.

(1S,2R,3R,4S,5S,6S)-4,5-bis(benzyloxy)-2-(hydroxymethyl)-7-oxabicyclo[4.1.0] heptan-3-ol (10) and (1R,2R,3R,4S,5S,6R)-4,5-bis(benzyloxy)-2-(hydroxymethyl)-7-oxabicyclo[4.1.0]heptan-3-ol (11)

To a solution of cyclohexene **9** (0.953 g, 2.8 mmol) in DCE (48 mL) was added *m*CPBA (55%) (1.32 g, 4.2 mmol) and the mixture was heated to reflux. After complete conversion of the starting material the mixture was cooled to room temperature and silica was added to the mixture after which the solvents were

removed *in vacuo*. The immobilized product was directly purified by column chromatography (1/1 → 3/7, pentane/EtOAc, v/v) yielding benzylated β-manno cyclophellitol **11** (0.283 g, 0.794 mmol, 29%) and benzylated α-manno cyclophellitol **10** (0.180 g, 0.505 mmol, 18%) both as a white amorphous solid.

(1S,2R,3R,4S,5S,6S)-4,5-bis(benzyloxy)-2-(hydroxymethyl)-7-oxabicyclo[4.1.0] heptan-3-ol (10)

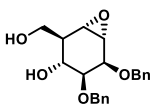

^{1}H NMR (400 MHz, $CDCl_3$) δ 7.40 – 7.27 (m, 10H), 4.83 (d, *J* = 12.0 Hz, 1H), 4.65 (d, *J* = 11.9 Hz, 1H), 4.62 (d, *J* = 11.6 Hz, 1H), 4.51 (d, *J* = 11.6 Hz, 1H), 4.28 (t, *J* = 2.9 Hz, 1H), 3.93 (dd, *J* = 9.8, 3.4 Hz, 1H), 3.91 (d, *J* = 10.2 Hz, 1H), 3.83 (dd, *J* = 10.7, 5.8 Hz, 1H), 3.53 (dd, *J* = 10.1, 3.1 Hz, 1H), 3.26 (t, *J* = 3.1 Hz, 1H), 3.07 (d, *J* = 3.6 Hz, 1H), 2.69 (s, 2H), 2.18 (dt, *J* = 8.8, 5.9 Hz, 1H). ^{13}C NMR (100 MHz, $CDCl_3$) δ 138.2, 137.8, 128.8, 128.6, 128.2, 128.1, 128.1, 128.0, 79.6, 74.0, 72.6, 71.6, 67.5, 63.7, 54.5, 53.7, 44.1. HRMS: found 357.1696 $[M+H]^+$, calculated for $[C_{21}H_{24}O_5+H]^+$ 357.1696.

(1R,2R,3R,4S,5S,6R)-4,5-bis(benzyloxy)-2-(hydroxymethyl)-7-oxabicyclo[4.1.0] heptan-3-ol (11)

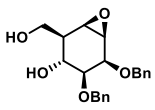

^{1}H NMR (600 MHz, $CDCl_3$) δ 7.45 – 7.41 (m, 2H), 7.39 – 7.27 (m, 8H), 4.85 (d, *J* = 12.1 Hz, 1H), 4.65 (d, *J* = 11.6 Hz, 1H), 4.63 (d, *J* = 12.1 Hz, 1H), 4.42 (d, *J* = 11.6 Hz, 1H), 4.10 – 4.05 (m, 2H), 3.93 (dd, *J* = 10.7, 5.1 Hz, 2H), 3.91 (t, *J* = 9.7 Hz, 1H), 3.28 (dd, *J* = 3.7, 2.0 Hz, 1H), 3.24 (dd, *J* = 4.9, 3.7 Hz, 1H), 3.20 (dd, *J* = 10.1, 5.0 Hz, 1H), 2.76 (s, 1H), 2.61 (s, 1H), 2.10 (dddd, *J* = 9.1, 7.1, 5.2, 2.0 Hz, 1H). ^{13}C NMR (151 MHz, $CDCl_3$) δ 137.8, 137.5, 128.7, 128.6, 128.5, 128.2, 128.1, 79.7, 71.5, 71.4, 68.5, 67.1, 64.5, 54.6, 50.4, 44.8. HRMS: found 357.1696 $[M+H]^+$, calculated for $[C_{21}H_{24}O_5+H]^+$ 357.1696.

(1R,2S,3S,4R,5R,6R)-2,3,4-tris(benzyloxy)-5-((benzyloxy)methyl)-7-oxabicyclo [4.1.0]heptane (12)

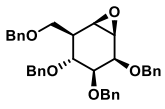

To a 0°C cooled solution of β-manno cyclophellitol **11** (0.104 g, 0.29 mmol) in DMF (2.9 mL) was added BnBr (86 µl, 0.725 mmol) and NaH (60%) (29 mg, 0.725 mmol) in small portions and the reaction mixture was allowed to warm to room temperature. After complete conversion of the starting material the mixture was cooled to 0°C and quenched with MeOH. The solvent was removed *in vacuo* and the crude was dissolved in Et_2O. The product was washed with H_2O (3x), brine (2x), dried over $MgSO_4$, filtered and concentrated *in vacuo*. Purification by column chromatography (7/3, pentane/Et_2O, v/v) yielded the product as a white amorphous solid (80.6 mg, 0.15 mmol, 52%). ^{1}H NMR (400

MHz, $CDCl_3$) δ 7.46 – 7.41 (m, 2H), 7.40 – 7.26 (m, 16H), 7.24 – 7.18 (m, 2H), 4.83 (d, *J* = 12.5 Hz, 1H), 4.79 (d, *J* = 11.2 Hz, 1H), 4.72 (d, *J* = 12.5 Hz, 1H), 4.60 (s, 2H), 4.56 (d, *J* = 12.1 Hz, 1H), 4.51 (d, *J* = 12.0 Hz, 1H), 4.42 (d, *J* = 11.2 Hz, 1H), 4.04 (t, *J* = 4.6 Hz, 1H), 3.77 (dd, *J* = 8.8, 4.9 Hz, 1H), 3.69 (t, *J* = 8.8 Hz, 1H), 3.60 (dd, *J* = 8.7, 7.6 Hz, 1H), 3.47 (dd, *J* = 4.8, 2.1 Hz, 1H), 3.46 (t, *J* = 4.9 Hz, 1H), 3.27 (t, *J* = 4.0 Hz, 1H), 2.30 (dddd, *J* = 8.8, 7.6, 4.9, 2.6 Hz, 1H). ^{13}C NMR (100 MHz, $CDCl_3$) δ 138.5, 138.5, 138.4, 138.3, 128.6, 128.5, 128.5, 128.5, 128.3, 128.2, 128.0, 128.0, 127.8, 127.8, 127.8, 127.7, 79.7, 74.4, 73.6, 73.4, 72.7, 71.5, 70.9, 69.4, 54.7, 52.0, 42.6. HRMS: found 537.2635 $[M+H]^+$, calculated for $[C_{35}H_{35}O_5+H]^+$ 537.2636.

(1S,2R,3S,4R,5R,6S)-2,3,4-tris(benzyloxy)-5-((benzyloxy)methyl)-7-azabicyclo [4.1.0]heptane (13)

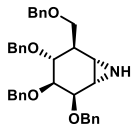

To a solution of **12** (53.7 mg, 0.1 mmol) in MeCN (2 mL) was added $LiClO_4$ (16 mg, 0.15 mmol), NaN_3 (65 mg, 1.0 mmol) and the reaction mixture was stirred overnight at 80°C under an argon atmosphere. The reaction mixture was cooled to room temperature and quenched with H_2O. The product was extracted with DCM (5x) from the water and the combined organic layers were dried over $MgSO_4$, filtered and concentrated *in vacuo*. The concentrated residue was dissolved in MeCN (3.3 mL) and PPh_3 polymer-bound on styrene-divinylbenzene copolymer (0.188 g, 0.564 mmol, 3 mmol/g) was added. After stirring at reflux conditions overnight, the reaction mixture was concentrated *in vacuo*. Purification over silica gel column chromatography (1% MeOH in DCM) gave cyclophellitol aziridine **24** (95.6 mg, 0.178 mmol, 54%) as yellow oil. ^{1}H NMR (400 MHz, $CDCl_3$) δ 7.42 – 7.17 (m, 20H), 4.93 (d, *J* = 12.3 Hz, 1H), 4.84 (d, *J* = 11.3 Hz, 1H), 4.76 – 4.57 (m, 3H), 4.55 – 4.34 (m, 3H), 4.21 (t, *J* = 2.2 Hz, 1H), 3.80 – 3.65 (m, 2H), 3.61 (dd, *J* = 9.1, 4.0 Hz, 1H), 3.50 (t, *J* = 8.7 Hz, 1H), 2.42 (dd, *J* = 5.8, 2.3 Hz, 1H), 2.33 (d, *J* = 5.8 Hz, 1H), 2.30 – 2.22 (m, 1H). ^{13}C NMR (101 MHz, $CDCl_3$) δ 139.2, 139.0, 139.0, 138.5, 128.4, 128.4, 128.3, 128.1, 127.8, 127.7, 127.6, 127.5, 127.5, 80.8, 75.6, 75.2, 74.7, 73.3, 73.0, 73.0, 70.9, 43.4, 34.5, 31.8. HRMS: found 536.2792 $[M+H]^+$, calculated for $[C_{35}H_{37}NO_4+H]^+$ 536.2795.

(1S,2R,3S,4R,5R,6S)-5-(hydroxymethyl)-7-azabicyclo[4.1.0]heptane-2,3,4-triol(14)

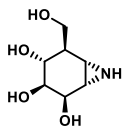

Liquid NH_3 (30 mL) was obtained by condensation of gas NH_3 at -60°C. Lithium (140 mg) was added and the mixture was stirred for 30 min, resulting in a dark blue solution. Aziridine **13** (149 mg, 0,278 mmol) was dissolved in THF (7 mL) and slowly added to the reaction mixture. After stirring for 75 min, the reaction was quenched with milliQ-H_2O (4 mL). The

solution was allowed to come to room temperature followed by concentrating *in vacuo*. The crude mixture was taken up in milliQ-H_2O and neutralized with Amberlite IR H^+. Product bound on the resin was washed with milliQ-H_2O followed by elution with NH_4OH (1M). The basic solution was concentrated *in vacuo* and dissolved again in milliQ-H_2O. Addition of Amberlite-NH_4^+, followed by elution with milliQ-H_2O and concentration *in vacuo* gave cyclophellitol aziridine **25** as clear oil which was used without further purification. ^{1}H NMR (400 MHz, D_2O) δ 4.34 (s, 2H), 3.89 (dd, *J* = 11.1, 3.4 Hz, 1H), 3.72 (dd, *J* = 10.9, 7.6 Hz, 1H), 3.51 – 3.42 (m, 2H), 2.50 (d, *J* = 5.5 Hz, 1H), 2.31 (d, *J* = 5.7 Hz, 1H), 1.87 (s, 1H). ^{13}C NMR (101 MHz, D_2O) δ 70.5, 68.3, 66.5, 62.0, 45.0, 35.2, 31.0. HRMS: found 176.0917 $[M+H]^+$, calculated for $[C_7H_{12}NO_4+H]^+$ 176.0917.

(1S,2R,3S,4R,5R,6S)-7-(8-azidooctyl)-5-(hydroxymethyl)-7-azabicyclo[4.1.0] heptane-2,3,4-triol (15)

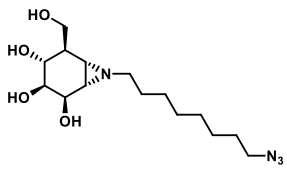

Compound **14** (66 mg, 0.2 mmol), 1-azido-8-iodooctane (67 mg, 0.24 mmol) and K_2CO_3 (118 mg, 0.86 mmol) in DMF (2 mL) was stirred at 80°C. After stirring overnight the reaction mixture was concentrated *in vacuo* and purification over silica gel column chromatography (12% MeOH in DCM) gave azide-cyclophellitol aziridine 3 (25.2 mg, 76 µmol, 38% over two steps) as clear oil. ^{1}H NMR (400 MHz, MeOD) δ 4.27 – 4.20 (m, 1H), 3.92 (dd, *J* = 10.6, 4.2 Hz, 1H), 3.62 (dd, *J* = 10.6, 8.4 Hz, 1H), 3.44 (dd, *J* = 10.2, 3.4 Hz, 4H), 3.38 (d, *J* = 9.2 Hz, 1H), 3.30 (t, *J* = 3.4 Hz, 2H), 2.38 – 2.23 (m, 2H), 1.89 – 1.81 (m, 2H), 1.73 (d, *J* = 6.1 Hz, 1H), 1.66 – 1.57 (m, 4H), 1.44 – 1.35 (m, 8H). ^{13}C NMR (101 MHz, MeOD) δ 72.8, 69.7, 68.2, 63.9, 61.8, 52.4, 47.0, 45.9, 41.7, 30.6, 30.2, 29.9, 28.3, 27.8. HRMS: found 329.2182 $[M+H]^+$, calculated for $[C_{15}H_{28}N_4O_4+H]^+$ 329.2183.

N-(9-(2-carboxy-4-((1-(1-(8-((1S,2R,3S,4R,5R,6S)-2,3,4-trihydroxy-5-(hydroxyl-methyl)-7-azabicyclo[4.1.0]heptan-7-yl)octyl)-1H-1,2,3-triazol-4-yl)-2,5,8,11-tetraoxatridecan-13-yl)carbamoyl)phenyl)-6-(dimethylamino)-3H-xanthen-3-ylidene)-N-methylmethanaminium (ABP 16)

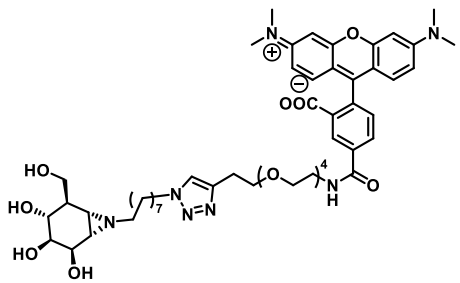

α-Mannose configured cyclophellitolaziridine azide (**15**) (6.3 mg, 19 µmol), CuI (0.4 mg, 1.9 µmol), THPTA (0.8 mg, 1.9 µmol) and **5** (5.0 mg, 7.8 µmol) were dissolved in DMF (0.4 ml) and stirred for 48 hours at room temperature. The mixture was purified by semi-preparative

HPLC follow by lyophilization affording the compound as a red solid (3.4 mg, 44%). ^{1}H NMR (850 MHz, D_2O) δ 8.21 (d, *J* = 1.9 Hz, 1H), 7.95 (dd, *J* = 7.7, 1.9 Hz, 1H), 7.78 (s, 1H), 7.32 (d, *J* = 7.8 Hz, 1H), 7.07 (d, *J* = 9.4 Hz, 2H), 6.76 (dd, *J* = 9.5, 2.5 Hz, 2H), 6.49 (d, *J* = 2.5 Hz, 2H), 4.45 (s, 2H), 4.20 (t, *J* = 2.3 Hz, 1H), 4.17 (t, *J* = 7.0 Hz, 2H), 3.78 (dd, *J* = 11.1, 3.8 Hz, 1H), 3.73 (t, *J* = 5.2 Hz, 2H), 3.70 – 3.66 (m, 2H), 3.66 – 3.63 (m, 2H), 3.63 – 3.59 (m, 4H), 3.57 (dd, *J* = 11.2, 7.7 Hz, 1H), 3.56 – 3.53 (m, 6H), 3.32 – 3.30 (m, 2H), 3.09 – 3.06 (m, 12H), 2.15 – 2.10 (m, 1H), 2.06 (ddd, *J* = 12.0, 8.2, 6.3 Hz, 1H), 1.80 (dd, *J* = 6.1, 2.0 Hz, 1H), 1.73 (ddd, *J* = 10.3, 7.9, 4.5 Hz, 1H), 1.62 (m, 3H), 1.34 – 1.27 (m, 2H), 1.08 – 0.96 (m, 8H). ^{13}C NMR (214 MHz, D_2O) δ 173.0, 169.3, 158.3, 157.0, 156.9, 143.7, 140.6, 135.1, 134.4, 130.8, 130.1, 128.1, 127.6, 124.6, 113.9, 112.7, 96.1, 71.1, 69.7, 69.7, 69.6, 69.6, 69.5, 68.9, 67.7, 66.2, 63.1, 61.9, 59.7, 50.3, 44.7, 44.0, 40.2, 40.0, 39.8, 29.2, 28.5, 28.4, 27.9, 26.3, 25.4. HRMS: found 486.7572 $[M+2xH]^{2+}$, calculated for $[C_{51}H_{69}O_{12}N_7+2xH]^{2+}$ 486.7577

Gel-Activity Based Protein Profiling experiments

Jack bean α-mannosidase was purchased from Sigma and used as supplied. Cell extracts from mouse testis were suspended in lysis buffer (20 mM Hepes, 0.25 M sucrose, pH 7.0). The mixture was homogenized using sonication. Samples were diluted in McIlvaine buffer (with a specific pH) supplemented with 1 mM $ZnCl_2$. Final protein content for jack bean mannosidase samples and mouse testis were respectively 1 and 5 µg (V_{final} = 20 µL). Lysates from mouse tissue were pre-incubated with 25 µM of **1** or DMSO for 30 minutes at 37°C. Probe concentration was equal to 5 µM for all samples and labelling was conducted for 30 minutes at 37°C. Protein content was subsequently denatured using Laemmli Buffer (4x) at 100°C for 3 minutes. Reactions were resolved by 12.5% SDS-PAGE electrophoresis and wet slabs were scanned for fluorescence (Molecular Imager Gel Doc XR, Biorad).

Purification of dGMII

Conditioned medium (3.6 L) was cleared of cells by centrifugation at 200 *g* for 15 min at 4°C, followed by further clearing of debris by centrifugation at 4,000 *g* for 45 min at 4°C. DTT (1 mM) and AEBSF (0.1 mM) were added to cleared medium, which was then loaded onto a 5 mL HisTrap excel column (GE Healthcare). The column was washed with 10 column volumes (CV) of buffer A (50 mM HEPES, pH 8.0, 0.5 M NaCl. 30 mM imidazole, 1 mM DTT) then eluted with a linear gradient of 0-100 % buffer B (50 mM HEPES, pH 8.0, 0.5 M NaCl. 1 M Imidazole, 1 mM DTT) over 20 CV. Fractions containing protein (as determined by SDS-PAGE) were pooled and diluted 5-fold with a 50 % mixture of buffer C (20 mM HEPES, pH 7.4 , 100 mM NaCl, 1 mM

DTT, pH 7.4) and de-ionized water. The pooled and diluted protein was then loaded onto a pre-equilibrated 5 mL HiTrap Blue HP column and washed with 20 CV buffer C. Protein was then eluted with a 0-100 % gradient of buffer D (20 mM HEPES, pH 7.4, 1M NaCl, 1 mM DTT, pH 7.4) over 20 CV. Fractions containing protein were then pooled and concentrated to < 1 mL with a 50-kDa Vivaspin concentrator. AcTEV protease (ThermoFischer) was added to the concentrated protein and this mixture was incubated at 20°C for 18 h, after which proteolysis was confirmed by SDS-PAGE. Digested protein was purified by size-exclusion chromatography (SEC) with a Superdex S200 16/600 column (GE Healthcare) in SEC buffer (50 mM HEPES, pH 7.4, 200 mM NaCl, 1 mM DTT). GMII-containing fractions were concentrated to 10 mg/mL with a 30-kDa Vivaspin concentrator and were buffer-exchanged into storage buffer (20 mM HEPES, pH 7.4, 20 mM NaCl, 1 mM DTT) through three rounds of dilution/re-concentration. Protein was flash frozen in liquid nitrogen and stored at –80°C until use.

Optimization and validation of the FluoPol-ABPP assay on dGMII

FluoPol-ABPP experiments were conducted in small volume 384-well black-bottom plates (Greiner). The optimal probe concentration on FluoPol signal was determined by varying probe concentrations from 1 nM to 100 nM at a constant dGMII concentration (100 nM) at pH = 6.5. Optimal pH was determined by preparation of different buffers, MES buffer for relatively high pH values and 100 mM acetate buffers for lower pH. These pH-experiments were performed at optimal probe concentration (25 nM). From there on all experiments were conducted in reaction buffer consisted of 20 mM MES, 1 mM $ZnSO_4$, 0.1 % BSA, 0.5 mg/mL Chaps at pH 6.5. Validation experiments were performed by varying the concentrations between 1 µM – 2 nM for **1** and 1 mM – 2 µM for **3**. For the competition experiments the enzyme and inhibitor were incubated at 37°C for 30 minutes prior to the addition of **16** to a final concentration of 25 nM. The FluoPol signal was determined using a CLARIOstar (BMG Labtech) plate reader at wavelengths λ_{ex} = 530 nm and λ_{em} = 580 nm after 18h incubation at 37°C. Negative controls contained DMSO in place of the inhibitor. All samples were corrected for background polarization, and the residual enzyme activity was calculated based on the polarization signal from the controls. IC_{50}-values were calculated via non-linear regression using GraphPad Prism 6.0 (N=2, n=3).

FluoPol-ABPP screen of the iminosugar library on dGMII

Screening of the iminosugar library was performed with the optimized conditions as described above. A final concentration of 5 µM of each compound in a 15 µL assay

was used for screening. Each screening plate contained negative controls (DMSO in place of compounds) and positive controls (**1** at 10 µM). Data was analyzed as above and the residual enzyme activities were plotted against the corresponding compound ID.

Analysis of selected compounds as inhibitors of dGMII

Competitive K_i values were determined at 25°C using a fixed concentration of substrate, 4-methylumbelliferyl α-D-mannoside (1 mM), and 50 nM dGMII in reaction buffer (50 mM MES, 1 mM $ZnSO_4$, 0.1 % BSA, pH 5.5). Inhibitor concentrations ranging from 0.2 to 5 times the K_i value ultimately determined. Continuous fluorescence measurements (λ_{ex} = 365 nm, λ_{em} = 450 nm) were made with a CLARIOstar Plus plate reader (BMG Labtech). Standards of 4-methylumbelliferone in reaction buffer were included in each assay plate. A horizontal line drawn through $1/V_{max}$ in a Dixon plot of these data (1/V vs [I]) intersects the experimental line at an inhibitor concentration equal to $-K_i$ All data were fit using the software program OriginPro (OriginLab Corporation).

Crystal formation of dGMII complexes with inhibtors

dGMII at 10 mg/mL was tested against a range of commercial crystallization screens. Large split crystals were found in several conditions of the JCSG+, PACT premier, index and PEG/ion screens, which were used for further optimization. Initial crystals were grown using the sitting-drop vapour-diffusion method at 20°C in 100 mM imidazole, pH 7.0 and 10% (w/v) PEG 3,350. These crystals were used to generate seeds that were used for rescreening the above libraries. Optimized dGMII crystals were grown in maxi 48-well plates using the sitting-drop vapour-diffusion method at 20°C with 100 mM succinate, pH 7.0, 10% (w/v) PEG 3,350 and a protein:seed:well solution ratio of 200:100:400 nL. Crystals were soaked in well solution containing 25% (v/v) ethylene glycol before flash cooling in liquid nitrogen. Inhibitor complexes were obtained by soaking crystals in well solution containing 1 mM of the inhibitor for 3-4 hours before flash cooling in liquid nitrogen.

5.5 References

(1) Shah, N., Kuntz, D. A., and Rose, D. R. (2008) Golgi -mannosidase II cleaves two sugars sequentially in the same catalytic site. *Proc. Natl. Acad. Sci. 105*, 9570–9575.

(2) Rose, D. R. (2012) Structure, mechanism and inhibition of Golgi α-mannosidase II. *Curr. Opin. Struct. Biol. 22*, 558–562.

(3) Dennis, J. W., Granovsky, M., and Warren, C. E. (1999) Protein glycosylation in development and disease. *BioEssays 21*, 412–421.

(4) Goss, P. E., Baker, M. A., Carver, J. P., and Dennis, J. W. (1995) Inhibitors of carbohydrate processing: A new class of anticancer agents. *Clin. Cancer Res. 1*, 935–944.

(5) Das, P. C., Roberts, J. D., White, S. L., and Olden, K. (1995) Activation of resident tissue-specific macrophages by swainsonine. *Oncol. Res. 7*, 425–433.

(6) Sun, J.-Y., Zhu, M.-Z., Wang, S.-W., Miao, S., Xie, Y.-H., and Wang, J.-B. (2007) Inhibition of the growth of human gastric carcinoma in vivo and in vitro by swainsonine. *Phytomedicine 14*, 353–359.

(7) Klein, J.-L. D., Roberts, J. D., George, M. D., Kurtzberg, J., Breton, P., Chermann, J.-C., and Olden, K. (1999) Swainsonine protects both murine and human haematopoietic systems from chemotherapeutic toxicity. *Br. J. Cancer 80*, 87–95.

(8) You, N., Liu, W., Wang, T., Ji, R., Wang, X., Gong, Z., Dou, K., and Tao, K. (2012) Swainsonine inhibits growth and potentiates the cytotoxic effect of paclitaxel in hepatocellular carcinoma in vitro and in vivo. *Oncol. Rep. 28*, 2091–2100.

(9) Mohla, S., White, S., Grzegorzewski, K., Nielsen, D., Dunston, G., Dickson, L., Cha, J. K., Asseffa, A., and Olden, K. (1990) Inhibition of growth of subcutaneous xenografts and metastasis of human breast carcinoma by swainsonine: modulation of tumor cell HLA class I antigens and host immune effector mechanisms. *Anticancer Res. 10*, 1515–1522.

(10) Olden, K., Breton, P., Grzegorzewski, K., Yasuda, Y., Gause, B. L., Oredipe, O. A., Newton, S. A., and White, S. L. (1991) The potential importance of swainsonine in therapy for cancers and immunology. *Pharmacol. Ther. 50*, 285–290.

(11) Micheloud, J. F., Marin, R., Colque-Caro, L. A., Martínez, O. G., Gardner, D., and Gimeno, E. J. (2017) Swainsonine-induced lysosomal storage disease in goats caused by the ingestion of Sida rodrigoi Monteiro in North-western Argentina. *Toxicon 128*, 1–4.

(12) Šesták, S., Bella, M., Klunda, T., Gurská, S., Džubák, P., Wöls, F., Wilson, I. B. H., Sladek, V., Hajdúch, M., Poláková, M., and Kóňa, J. (2018) N-Benzyl substitution of polyhydroxypyrrolidines: the way to selective inhibitors of golgi α-mannosidase II.

ChemMedChem 13, 373–383.

(13) Li, B., Kawatkar, S. P., George, S., Strachan, H., Woods, R. J., Siriwardena, A., Moremen, K. W., and Boons, G.-J. (2004) Inhibition of golgi mannosidase II with mannostatin a analogues: synthesis, biological evaluation, and structure-activity relationship studies. *ChemBioChem 5*, 1220–1227.

(14) Popowycz, F., Gerber-Lemaire, S., Demange, R., Rodriguez-García, E., Asenjo, A. T. C., Robina, I., and Vogel, P. (2001) Derivatives of (2R,3R,4S)-2-aminomethylpyrrolidine-3,4-diol are selective α-mannosidase inhibitors. *Bioorg. Med. Chem. Lett. 11*, 2489–2493.

(15) Kuntz, D. A., Tarling, C. A., Withers, S. G., and Rose, D. R. (2008) Structural analysis of golgi α-mannosidase II inhibitors identified from a focused glycosidase inhibitor screen. *Biochemistry 47*, 10058–10068.

(16) Alonso-Gil, S., Males, A., Fernandes, P. Z., Williams, S. J., Davies, G. J., and Rovira, C. (2017) Computational design of experiment unveils the conformational reaction coordinate of GH125 α-mannosidases. *J. Am. Chem. Soc. 139*, 1085–1088.

(17) Kallemeijn, W. W., Li, K.-Y., Witte, M. D., Marques, A. R. a, Aten, J., Scheij, S., Jiang, J., Willems, L. I., Voorn-Brouwer, T. M., van Roomen, C. P. A. A., Ottenhoff, R., Boot, R. G., van den Elst, H., Walvoort, M. T. C., Florea, B. I., Codée, J. D. C., van der Marel, G. A., Aerts, J. M. F. G., and Overkleeft, H. S. (2012) Novel activity-based probes for broad-spectrum profiling of retaining β-exoglucosidases in situ and in vivo. *Angew. Chem. Int. Ed. 51*, 12529–12533.

(18) Tropea, J. E., Kaushal, G. P., Pastuszak, I., Mitchell, M., Aoyagi, T., Molyneux, R. J., and Elbein, A. D. (1990) Mannostatin A, a new glycoprotein-processing inhibitor. *Biochemistry 29*, 10062–10069.

(19) Kuntz, D. A., Nakayama, S., Shea, K., Hori, H., Uto, Y., Nagasawa, H., and Rose, D. R. (2010) Structural investigation of the binding of 5-substituted swainsonine analogues to golgi α-mannosidase II. *ChemBioChem 11*, 673–680.